Digest Journal of Nanomaterials and Biostructures Vol. 9, No. 4, October - December 2014, p. 1505 - 1511

INVESTIGATION OF InN NANOROD-BASED EGFET pH SENSORS FABRICATED ON QUARTZ SUBSTRATE

S. X. CHEN, S. P. CHANG*, S. J. CHANG
Institute of Microelectronics and Department of Electrical Engineering, Center for Micro/Nano Science and Technology, Advanced Optoelectronic Technology Center, National Cheng Kung University, Tainan 70101, Taiwan

The extended gate field effect transistor (EGFET) consists of an ion-sensitive electrode and a metal-oxide semiconductor field-effect-transistor (MOSFET) device. It can be used to measure ion content in an electrolytic solution. In this article, we present the work of our research group, which has successfully fabricated the first Indium Nitride (InN) nanorod as a sensitive membrane of the EGFET pH sensor. The InN nanorod-based EGFET pH sensor was fabricated on a quartz substrate using molecular beam epitaxy (MBE). The EGFET pH sensor with InN nanorods demonstrated improved sensing performance. The measured current and voltage sensitivities of the pH sensor were 26 μA/pH and 22.66 mV/pH, at pH values ranging from 4 to 10. This makes them suitable for a variety of applications such as pH sensors and biosensors.

(Received September 15, 2014; Accepted November 22, 2014)

Keywords: InN; nanorods; EGFET; pH sensors; MBE; quartz substrate

1. Introduction

The first ion-sensitive field effect transistor (ISFET) was presented by Bergveld, at the University of Twente, as the first chemical sensor using a semiconductor device [1]. Its basic design comprised an electrolyte and a SiO_2 sensing film that substituted the traditional metal gate to form the electrolyte-insulator-semiconductor structure. Developing this device would make an accurate pH sensor possible. The reliability of traditional ISFET was considerably affected by the impurities in chemical solutions that could puncture the FET. This disadvantage could be avoided by separating the device part and the sensing part. Therefore, many variations of the ISFET have been developed over recent decades [2-6]. The extended-gate field-effect transistor (EGFET), based on the ISFET operation principle, splits the original ISFET into two parts. The FET is isolated from the chemical solutions, and the sensing film is connected to the signal line extended from the FET electrode. Moreover, the EGFET is simple to package and is insensitive to light.

With the development of robust sensors, there is a growing trend towards the use of disposable sensors in medical applications. Recently, biosensors and pH sensors have been used by the medical community [7-9]. Extended-gate field-effect-transistor (EGFET) pH sensors are especially popular because they are inexpensive, easy to manufacture, highly responsive, extremely convenient, and very stable with regard to light and outside temperature [10-13]. Such advantages make them ideal for use in disposable detection devices. The EGFET pH sensor is composed of a MOSFET and a sensing film. Following increasing interest in EGFETs, we have investigated several thin-film materials and presented our results in earlier publications [14-16].

Concerted efforts have been made to research the characteristics of III–V group materials such as AlN, GaN, GaAs, InN, and InP in the past few years with success. InN, one of the candidate materials, has a high absorption coefficient, high carrier mobility, high drift velocity,

*Corresponding author: changsp@mail.ncku.edu.tw

and narrow direct band gap, making it suitable for optoelectronic and electronic applications [17-21]. Therefore, InN is a potential candidate for use in nanoscale devices such as photodetectors, gas sensors, and pH sensors. In EGFETs, the deposition of InN nanorods can improve the sensitivity more effectively than thin films, because nanorods have a higher surface-to-volume ratio and the sensitivity of pH sensors is a surface-sensing function [22-24]. It is possible to achieve high-quality crystalline InN nanorods with large-area growth methods. In this work, we study the performance of an EGFET pH sensor fabricated with 1-D InN nanorods and analyze its material, optoelectronic, and electronic characteristics.

2. Experimental Details

2.1. Fabrication of InN Nanorod-Based EGFET pH Sensor

Prior to growing nanorods, the substrate was sequentially cleaned with acetone, ethanol, and deionized (DI) water in an ultrasonic cleaner. An AlN buffer-layer of 80 nm was deposited on the substrate at 890 °C (K-cell temperature of Al source was 1190 °C) using MBE. InN nanorods were grown under In-rich conditions at 450 °C (K-cell temperature of In source was 735 °C). The substrate was exposed to a nitrogen flux of 1.2 sccm for 4 h at an RF-plasma power density of 12 mW/cm^3, while the chamber pressure was 10^{-9} Torr. The detailed process procedures for growing InN nanorods can be found elsewhere [25-27].

2.2. Methods of Measurement

Images of the surface morphology of InN nanorods were obtained using a field-emission scanning electron microscope (FESEM, JSM-7000F) at 10 keV. The crystalline properties of nanorods were measured using an X-ray scattering system with the X-17B1 beamline at the National Synchrotron Radiation Research Center (NSRRC) in Hsinchu, Taiwan. A photoluminescence (PL) measurement was taken in the infrared (IR) region, during which an Ar+ laser (488 nm) was used as the excitation source. The emission from InN nanorods was detected by an InGaAs detector and resolved using a spectrometer. The performance of the InN nanorod-based EGFET pH sensor was measured by the system shown as Figure 1. First, we connected the sensor's sensing region, which is the extended part of the gate, to the gate of the MOSFET. The sensor and an Ag/AgCl reference electrode were then immersed in the electrolytic solution, with the sensor and reference electrode connected to the measurement system. The sensor's response was analyzed using Agilent 4156C.

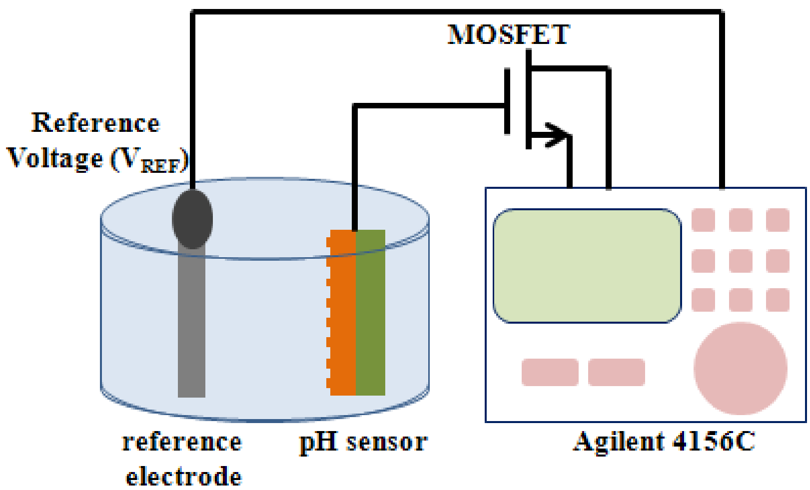

Fig. 1. Schematic diagram of an Indium Nitride (InN) nanorod pH sensor measurement system.

3. Results and Discussion

Fig. 2 shows FESEM images of the InN nanorod topology. High-density InN nanorods, of primarily (0002) orientation, were grown. It is suggested that by exposing the In thin film to a nitrogen (N_2) flux, large-area and low-cost growth of InN nanorods can be achieved. The hexagonal shape of nanorods is probably the result of the wurtzite structure of InN crystals.

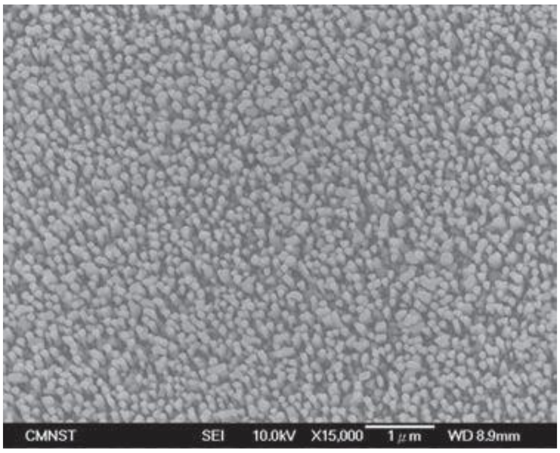

Fig. 2. Top view field-emission scanning electron microscope (FESEM) images of vertically aligned InN nanorods on a glass substrate.

The drain–source current (I_{DS}) of the InN nanorod-based EGFET is a function of the drain–source voltage (V_{DS}), when the reference electrode is at 3 V. Figure 3 illustrates that higher electrolytic solution pH value leads to lower I_{DS}, because higher pH implies that more OH^- ions can be found in an alkaline solution. However, these ions are equivalent to negative voltage acting on the EGFET, while connecting to the MOSFET. Therefore, the increase in OH^- ions results in smaller I_{DS}. Figure 4 shows the I_{DS} versus reference voltage (V_{REF}) characteristic curve of the InN nanorods EGFET pH sensor at V_{DS} = 0.3 V. It can be seen that increasing V_{REF} results to higher $I_{DS.}$ The dissociation of OH^- ions increases as V_{REF} grows, that is to say, the current rise when the V_{REF} increases.

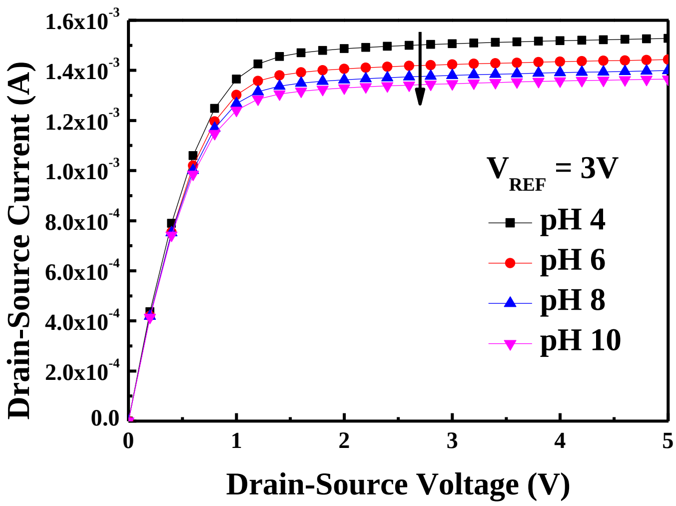

Fig. 3. Drain–source current–drain–source voltage characteristics of extended gate field effect transistor (EGFET) with an InN nanorods

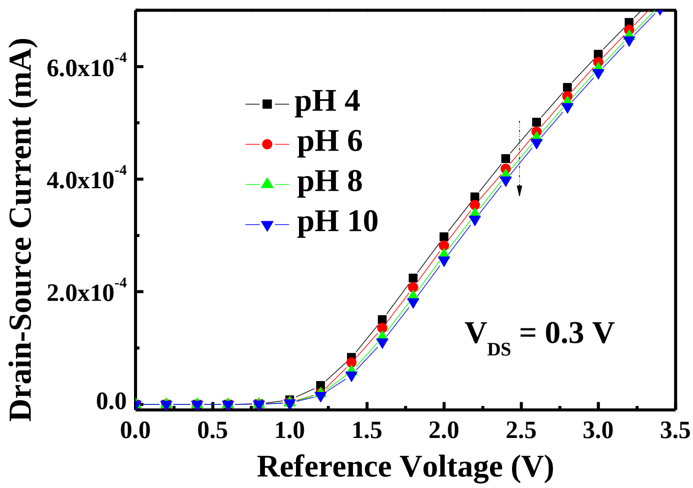

Fig. 4. Drain–source current–reference voltage characteristics of EGFET with an InN nanorod

Fig. 5 shows the relationship between V_{REF} and the pH value measured by the sensor. We observe that V_{REF} increases when the pH value increases. We can define the positive correlation between these two parameters as voltage sensitivity, which appears to be almost linear. The voltage sensitivity of the InN nanorod-based EGFET pH sensor is 22.66 mV/pH. An increase in the pH value and the number of OH^- ions leads to a negative bias on the gate, thus reducing I_{DS}. To maintain the value of I_{DS}, V_{REF} needs to go up when the pH value increases.

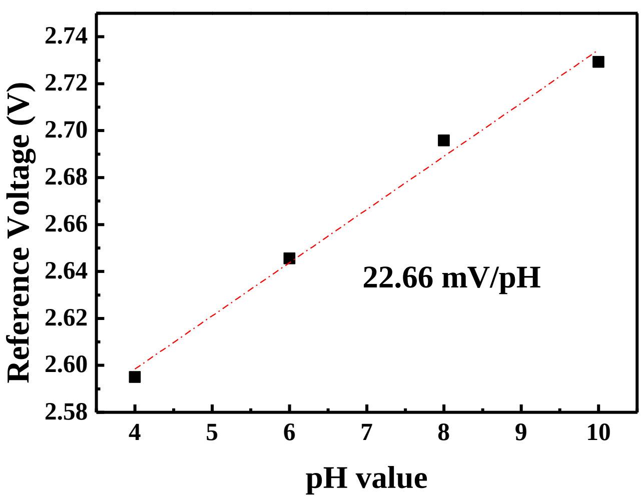

Fig. 5. Reference voltage–pH characteristics EGFET with an InN nanorod

There exists negative correlation between I_{DS} and the pH value, measured by the InN nanorod-based EGFET pH sensor as shown in Figure 6. The voltage V_{REF} was kept at 3 V, as defined by the current sensitivity. The current sensitivity of the EGFET pH sensor is 26 μA/pH. The sensor's H^+ ions accumulate on the surface when the pH value is low, resulting to a positive gate bias and an increase in I_{DS}. This approximate linear relationship indicates that I_{DS} changes because of the variation in the pH value of the solution. Thus demonstrating that the fabricated sensor could be used for pH measurements. This characteristic makes it possible to use the InN nanorods pH sensors not only for V_{REF} sensitivity, but also for I_{DS} sensitivity.

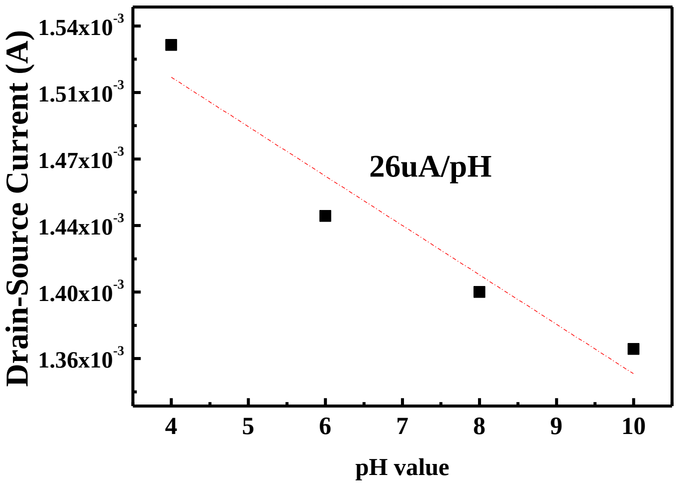

Fig. 6. Drain–source current–pH value characteristics EGFET with an InN nanorod

According to the site binding theory, the surface voltage of the extended gate changes with the pH of the electrolytic solution [28-29]. The surface potential voltage (ψ_o) between the sensing layer and the solution can be expressed as [30]:

$$2.303\left(pH_{pzc} - pH\right) = \frac{q\psi_0}{kT} + sinh^{-1}\left(\frac{q\psi_0}{kT} \cdot \frac{1}{\beta}\right), \tag{1}$$

where pH_{pzc} indicates the pH value at the point of zero charge, q is the charge of the electron, k is Boltzmann's constant, and T is the absolute temperature. The relationship between the surface sites per unit area (NS) and β can be expressed as Eq.2 [30]:

$$\beta = \frac{2q^2 N_S (K_a K_b)^{1/2}}{kTC_{DL}}, \tag{2}$$

where K_a is the acid equilibrium constant, K_b is the basic equilibrium constant, and CDL is the capacitance of the electrical bilayer derived by the Gouy–Chapman–Stern model [31]. With a larger sensitivity parameter β, better linear response between the surface potential voltage and the pH value could be derived from Eq.1. Generally speaking, Eq.1 and Eq.2 are the ideal models without surface states and dangling bonds. In fact, there are many dangling bonds and surface states on the surface of the InN nanorods. Indium (In), as an amphoteric metal, can interact with either an acidic or an alkaline solution. The surface chemistry of hydrous InN would be protonated or deprotonated in the electrolytic solution. The pH value of the solution is changeable because of the surface reaction between H^+ ions and InN. The surface charge of H^+ ions results in the production of OH^- or H^+ ions by protonation or deprotonation of the InN. As discussed above, the InN nanorod-based EGFET pH sensor already has good sensitivity to pH. However, in order to improve the pH sensor's sensitivity, the influence of the sensing surface area and the resulting capacitance should be taken into consideration.

4. Conclusion

In this study, we have presented the first InN nanorod-based EGFET pH sensor, which is easy to fabricate and use for measurement. As discussed in the article, the drain–source current (I_{DS}) and the reference voltage (V_{REF}) are positively correlated and negatively correlated with pH value. The InN nanorod-based EGFET pH sensor exhibits improved sensing performance, resulting from the enlarged sensing area and the surface-to-volume ratio, implying that the use of

InN nanorods for sensing is highly feasible and effective. We believe that InN nanorod-based pH sensors, with their excellent characteristics, will be extremely useful in pH sensing applications.

Acknowledgement

The authors would like to thank the National Science Council and Bureau of Energy, Ministry of Economic Affairs of Taiwan, R.O.C., for the financial support under Contract No. 103-2221-E-006-098 and 102-E0603, and the LED Lighting Research Center of NCKU for assisting with the device characterization. This work was also supported in part by the Center for Frontier Materials and MicroNano Science and Technology, the National Cheng Kung University, Taiwan, as well as by the Advanced Optoelectronic Technology Center, the National Cheng Kung University, under projects from the Ministry of Education.

References

[1] P. Bergveld, IEEE Trans. Biomed. Eng. **17**, 70 (1970).
[2] L. T. Yin, Study of Biosensors Based on an Ion Sensitive Field Effect Transistor. Diss. Chung Yuan Christian University. (2000).
[3] M. J. Schöning, Sensors **5**, 126 (2005).
[4] S. Middelhoek, Sens. Actuator B-Chem. **82**, 2 (2000).
[5] L. T. Yin, J. C. Chou, W. Y. Chung, T. P. Sun, and S. K. Hsiung, Sens. Actuator B-Chem. **71**, 106 (2000).
[6] J. C. Chou, P. K. Kwan, and Z. J. Chen, Jpn. J. Appl. Phys. **42**, 6790 (2003).
[7] L. L. Chi, L. T. Yin, J. C. Chou, W. Y. Chung, T. P. Sun, K. P. Hsiung, S. K. Hsiung, Sens. Actuator B-Chem. **71**, 68 (2000).
[8] P. T. Snee, R. C. Somers, G. Nair, J. P. Zimmer, M. G. Bawendi, D. G. Nocera, J. Am. Chem. Soc. **128**, 13320 (2006).
[9] B. S. Kang, H. T. Wang, F. Ren, S. J. Pearton, T. E. Morey, D. M. Dennis, J. W. Johnson, P. Rajagopal, J. C. Roberts, E. L. Piner, and K. J. Linthicum, Appl. Phys. Lett. **91**, 1 (2007).
[10] L. T. Yin, Y. T. Lin, Y. C. Leu, and C. Y. Hu, Sens. Actuator B-Chem. **148**, 207 (2010).
[11] S. P. Chang, C. W. Li, K. J. Chen, S. J. Chang, C. L. Hsu, T. J. Hsueh, H. T. Hsueh, Sci. Adv. Mater. 4, 1 (2012).
[12] S. P. Chang, and T. H. Yang, Int. J. Electrochem. Sci. **7**, 5020 (2012).
[13] Y. S. Chiu, C. Y. Tseng, and C. T. Lee, IEEE Sens. J. **12**, 930 (2012).
[14] P. Y. Lee, S. P. Chang, P. J. Kuo, E. H. Hsu, S. J. Chang, and S. C. Shei, Int. J. Electrochem. Sci. **8,** 3866 (2013).
[15] C. H. Kao, H. Chen, J. C. Wang, Y. C. Chu, C. S. Lai, S. P. Lin, C. Y. Huang, J. C. Ou, J. New Mat.Electrochem. Syst. **17**, 13 (2014).
[16] P. C. Yao, J. L. Chiang, and M. C. Lee, Solid State Sci. **28**, 47 (2014).
[17] A. F. d. Silva, J. F. D. Chubaci, M. Matsuoka, J. A. Freitas, Jr., J. G. Tischler, G. Baldissera, C. Persson, Phys. Status Solidi C. **11**, 581 (2014).
[18] J. J. Williams, T. L. Williamson, M. A. Hoffbauer, Y. Wei, N. N. Faleev, C. Honsberg, Phys. Status Solidi C. **11**, 577 (2014).
[19] K. Wang, T. Araki, M. Takeuchi, E. Yoon, and Y. Nanishi, Appl. Phys. Lett. **104**, 032108 (2014).
[20] V. Prozheeva, F. Tuomisto, G. Koblmüller, J. S. Speck, A. Knübel, R. Aidam, Phys. Status Solidi C. **11**, 530 (2014).
[21] Z. Bi, D. Lindgren, J. Johansson, M. Ek, L. R. Wallenberg, A. Gustafsson, M. T. Borgström, B. J. Ohlsson, B. Monemar, and L. Samuelson, Phys. Status Solidi C. **11**, 421 (2014).
[22] M. H. Huang, S. Mao, H. Feick, H. Yan, Y. Wu, H. Kind, E. Weber, R. Russo, P. Yang, Science **292**, 1897 (2001).
[23] Z. W. Pan, Z. R. Dai, and Z. L. Wang, Science **291**, 1947 (2001).
[24] Y. H. Chang, C. M. Liu, C. Chen, H. E. Cheng, J. Electrochem. Soc. **159**, D401 (2012).

[25] K. H. Lee, S. P. Chang, K. W. Liu, P. C. Chang, S. J. Chang, T. P. Chen, H. W. Shiu, L. Y. Chang, C. H. Chen, Int. J. Electrochem. Sci. **8**, 3212 (2013).
[26] K. H. Lee, S. P. Chang, K. W. Liu, P. C. Chang, S. J. Chang, T. P. Chen, H. W. Shiu, L. Y. Chang, C. H. Chen, Sci. Adv. Mater. **5**, 1 (2013).
[27] S. P. Chang, S. Wang, Dig. J. Nanomater. Biostruct. **9**, 929 (2014).
[28] D. E. Yates, S. Levine, and T. W. Healy, J. Chem. Soc., Faraday Trans. **1**(70), 1807 (1974).
[29] R. E. G. van Hal, J. C. T. Eijkel, P. Bergveld, Sens. Actuator B-Chem. **24**, 201 (1995).
[30] H. K. Liao, L. L. Chi, J. C. Chou, W. Y. Chung, T. P. Sun, and S. K. Hsiung, Mater. Chem. Phys. **59**, 6 (1999).
[31] K. B. Oldham, J. Electroanal. Chem. **613**, 131 (2008).